In Situ Investigation of the Deactivation Mechanism in Ni-ZSM5 During Ethylene Oligomerization

(Article begins on next page)

07 January 2023

In situ investigation of the deactivation mechanism in Ni-ZSM5 during ethylene oligomerization

Ganjkhanlou Y[1,2], Berlier G[1], Groppo E[1], Borfecchia E[1] and Bordiga S*[1,3]

1-Dipartimento di Chimica, NIS Centre of Excellence and INSTM Università di Torino, Via P. Giuria 7, 10125 Turin, Italy
2-Department of Physical Chemistry, Faculty of Chemical Technology, University of Pardubice, Studentská 573, CZ-53210 Pardubice, Czech Republic
3- Dept. of Chemistry, University of Oslo, Oslo, Norway

Abstract. Ethylene oligomerization reaction on Ni-modified and unmodified ZSM-5 catalysts was studied at ambient pressure as a function of temperature by *in situ* FT-IR spectroscopy and mass spectrometry, focusing the attention on the formation of adsorbed species, which are likely to be responsible for the catalysts deactivation. The two catalysts show similar catalytic performance and selectivity, but different stability with time-on-stream, particularly in the 300-400 °C range. On both catalysts alkylated compounds and unsaturated carbocations stable up to 300 °C, were observed as stable adsorbed species. The deactivation of the Ni-ZSM5 catalyst was related to the formation of a complex mixture of methylated polycondensed aromatic compounds (coke/coke precursors), which are not desorbed even by increasing the temperature up to 400 °C. In contrast, at 400 °C ethylene oligomerization on H-ZSM5 sample proceeds without deactivation due to the higher desorption rate of the surface species, which are mainly unsaturated carbocations with small amounts of methylated poly-condensed aromatics.

Keyword: In situ spectroscopy, Deactivation, Catalyst, Oligomerization, Nickel.

Introduction

Ethylene oligomerization is one of the major processes for producing linear and branched higher alkenes used in plastics, lubricants and surfactants [1-4]. Industrially, the process is performed using organometallic complexes as homogeneous catalysts in organic solvents [5-9], while heterogeneous catalysts generally display a lower activity that limits their practical application. Acidic zeolites (such as H-ZSM5) are well known catalysts for ethylene oligomerization [10], with high affinity toward light olefins since the kinetic diameters of common light alpha olefins [e.g. butene (0.45-0.50 nm), propene (0.43-0.45 nm)] [11,12] and ethylene (0.41-0.43 nm) [13] are in the range of the pore diameter of many zeolites (0.56 x 0.53 nm for H-ZSM5) [14,15]. The characteristics of the zeolite, such as pore size and Lewis and Brønsted acid sites ratio [7,16], have profound effects on the outcome of the reaction. Typically, the optimum temperature is in the range

of 50-150 °C and the operation pressure is about 2-10 MPa (20-100 atm) [7,16,17]. Catalytic tests carried out at ambient pressure on H-ZSM-5 were reported by Lin et al., who worked at higher temperature (optimum around 300 °C) [18]. Besides low activity, the main limitation of acidic zeolites is related to poor selectivity, because the reaction proceeds through a carbocationic mechanism.

Presently, Ni-modified inorganic porous materials are gaining interest as potential heterogeneous catalysts for selective ethylene oligomerization [19], although they still suffer for deactivation at high temperature. Interestingly, ethylene oligomerization on Ni containing zeolites occurs without the need of an activator, while other counterparts (e.g. titanium and chromium-based catalysts) need it to have satisfactory yield [2,9,20]. Ethylene oligomerization over Ni modified zeolites has been the subject of numerous investigations [3,19,21], mainly related to the evaluation of the catalytic activity and to the understanding of the reaction mechanism through the use of DFT calculations [10,17,19], whereas the mechanism of catalyst deactivation has been rarely addressed in the literature. During ethylene oligomerization in the presence of Ni cations different carbonaceous species are formed [22-24], which remain adsorbed on the catalyst surface also at high reaction temperature, affecting the selectivity and the reactivity of the catalyst. It is clear that identifying the types of species adsorbed at the surface of the catalyst is fundamental to understand the mechanism of the catalyst deactivation.

In this work, we investigate ethylene oligomerization over Ni free and Ni modified H-ZSM5 zeolites as a function of temperature, combining *in situ* Fourier-Transform Infrared (FT-IR) spectroscopy and mass spectrometry (MS) techniques. *In situ/operando* FT-IR spectroscopy is an advanced powerful technique which allows determining the different adsorbed species formed on the catalyst surface under working or similar condition [25,26], while MS technique allows to monitor the outcome of the oligomerization reaction. Combination of the two techniques permits to understand the mechanism of catalyst deactivation. A similar approach was previously proposed by Stepanov et al [27], who analysed the adsorbed species formed on the H-ZSM5 catalyst upon interaction with ethylene at ambient temperature. However, ethylene oligomerization at ambient pressure is usually performed at higher temperature [18]. Thus, in this work the ethylene conversion between 150 and 400 °C at ambient pressure was studied, with particular attention to the formation of adsorbed species. Even if the used set-up does not allow us to work in proper *operando* conditions (with catalytic results not directly comparable with the literature), we believe that the reported spectroscopic results are new with respect to the literature, and can give precious information for a better understanding of deactivation process, in relation to Brønsted and metal ions sites.

Experimental

Materials

Commercially available microsized H-ZSM5 material (Zeochem International: PZ-2/100H, Si/Al = 59) was utilized as starting materials. Ni was added to the sample by impregnation method. This process was carried out by dissolving 0.5 g of nickel acetylacetonate ($[Ni(acac)_2]_3$, where acac is the anion $C_5H_7O_2^-$) in 20 mL of toluene. 5 g of zeolite was added to the solution, stirred at room temperature for 30 min and toluene was then evaporated in a rotary evaporator. The corresponding Ni loading was 2 wt% (confirmed by EDS analysis). Next, the sample was calcined in air flow from room temperature to 550 °C, and left at this temperature for 6 hours. The resulting catalyst is hereafter labelled as Ni-ZSM5. The nature of the Ni sites present in the sample has been the subject of our recent spectroscopic investigation, showing the presence of a variety of Ni species, including exchanged (counterions) and grafted Ni^{2+} and small NiO particles [28].

Techniques

For the *in situ* FT-IR measurements, ~10 mg of each catalyst were pressed into self-supporting pellets and placed inside a commercial FT-IR reactor cell (AABSPEC, no. 2000-A multimode), which allows recording of infrared spectra under controlled temperature and gas atmosphere. A standard procedure is shown in Figure 1. Prior to the measurements, the catalysts were heated up to 400 °C (heating rate 5 °C/min) in oxygen flow (50 mL/min). After 30 min, the samples were flushed with He (50 ml/min) at the same temperature, followed by cooling down to 150 °C. A FT-IR spectrum was collected in these conditions. At this point, the temperature was increased in three steps from 150 to 400 °C and at each temperature the reactivity was studied by sending two pulses of ethylene/He mixture (20/50 ml/min) of 10 minutes each, followed by 5 minutes pulse of He (50 ml/min). The FT-IR spectra were recorded every 5 min during heating and cooling down, and every minute during the C_2H_4 and He pulses. Spectra obtained in the two consecutive pulses in the same gas did not show appreciable differences. For each temperature, the spectra are reported after subtracting the spectrum measured at the same temperature in He flow during the cooling step. The FT-IR spectra were recorded in transmission mode, at a resolution of 2 cm^{-1}, on a PerkinElmer System 2000 infrared spectrophotometer equipped with a MCT detector. Simultaneous MS data were recorded by a Thermo VG Smart IQ$^+$ instrument, coupled with the FT-IR spectrometer.
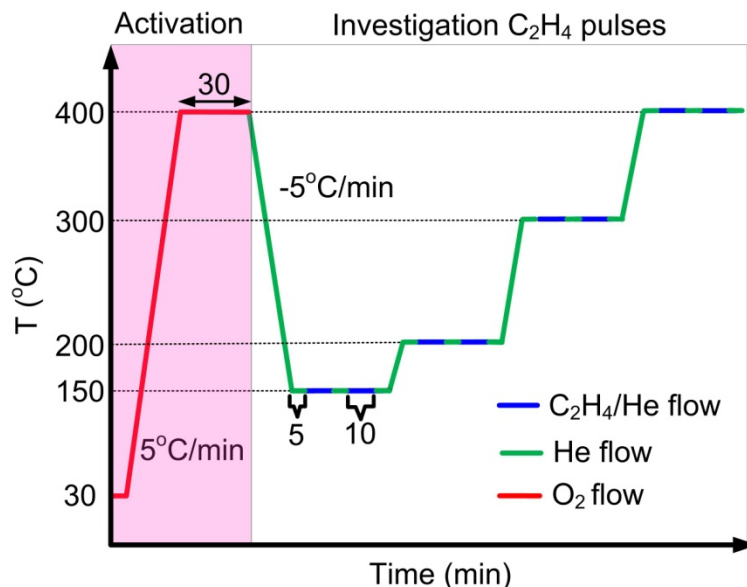
Figure 1. Temperature program utilized for the activation of the catalysts and the successive catalytic tests.

Results and discussion

The FT-IR spectra recorded under ethylene and helium flow at different temperatures are reported in Figure 2 and Figure 3 for H-ZSM5 and Ni-ZSM5 samples, respectively. For both samples the spectra measured during ethylene flow (both pulses) are plotted in the left hand panels, while those obtained while flushing helium are on the right hand. All high frequency regions (panels a, c, e and g) and low frequency ones (b, d, f, h) are plotted for each sample in the same vertical scale, for direct comparison. Different vertical scales were chosen for the two spectral regions to better appreciate small changes and weak feature in the bending region, which is intrinsically characterized by lower intensity. In all panels, the first measured spectrum at each temperature is plotted in black, intermediate spectra are in grey and the last one (after 10 or 5 minutes in ethylene or He, respectively) in different colours for each temperature. Generally speaking, the FT-IR spectra collected during ethylene flow show the signals of ethylene in the gas phase (indicated by coloured labels) combined with the spectroscopic features of the adsorbed species. The spectrum of gas phase ethylene is the main species observed on the first spectra collected at 150 °C, which is reported as black curves in Figures 2a) and 3a). In contrast, upon switching to pure helium flow the signals of gas phase ethylene disappear, making more evident the absorption bands due to the stable adsorbed species.

Starting the discussion from H-ZSM5 (Figure 2), under ethylene flow at 150 °C, some absorption bands related to saturated hydrocarbons (alkanes) appear and evolve as a function of time (Figure 2a). More in detail, the bands at 2958 and 2873 cm^{-1} (shoulder) are assigned to the ν_{asym} and ν_{sym} vibrational modes of CH_3 groups, while those at 2930 and 2860 cm^{-1} are assigned to the ν_{asym} and ν_{sym} modes of CH_2 groups, respectively [29,30]. In the low frequency region the corresponding bending modes of CH_3 (δ_{asym} at 1469 cm^{-1} and δ_{sym} at 1387 cm^{-1}) and CH_2 (shoulder

at 1455 cm^{-1}) groups are observed [30]. These bands are partially overlapped to the signals related to ethylene gas phase (black curve) at 2960 and 1419 cm^{-1} in left and right panels, respectively. Very weak features are also observed at 1597, 1537 and 1505 cm^{-1}, which will be discussed in more detail in the following. At the same time, unsaturated hydrocarbons are detected by MS (see below). Moreover, the absorption band related to the Brønsted sites (3600-3602 cm^{-1}) disappears (negative bands in the background subtracted spectra, vide infra Figure 4). Since there is no evidence for adsorbed ethylene (which could interact with Brønsted sites through π electrons) this could be interpreted as the formation of protonated species, as discussed by Pazè et al. [31].

What we observe by infrared spectroscopy in these conditions cannot be explained on the basis of adsorbed oligomers (reaction intermediates or products, which are released from the catalyst surface and detected by MS), since no signals are observed in the typical range of alkenes ν(CH$_x$) (above 3000 cm^{-1}, apart from ethylene gas phase in left panels). This is at variance with what observed by Bolis et al. on H-ZSM-5 [32], or by Groppo et al. who studied ethylene polymerization on the Phillips catalyst [33]. Noticeably, both authors studied the *in situ* reactivity of ethylene in static conditions, so that the observed spectral features could be assigned to the first stages of the oligomerization or polymerization reaction. On the contrary, what we observe in flow conditions can be assigned to stable adsorbed species, that is by-products which are likely to be responsible for the catalysts deactivation. On the other hand, our results are similar to what observed by Trombetta et al., who studied the isomerization of butene on H-ZSM-5 [34]. In agreement with these authors, we explain the observed features in terms of highly saturated hydrocarbons, formed as a result of ethylene condensation. The asymmetric character of the δ(CH$_3$) band at 1378 cm^{-1} (with a component at 1368 cm^{-1}) clearly show that a fraction of carbon atoms are bonded to two methyl groups [31]. These compounds are not desorbed by the catalyst surface under He flow up to 200 °C (Figures 2b, 2d and right panel of Figure 4a). We cannot exclude the hypothesis that these are (at least in part) protonated, due to the disappearance of the band due to Brønsted sites.

At 200 °C in ethylene flow bands at 1957 and 1505 cm^{-1} (with a shoulder at 1537 cm^{-1}) become evident. The former immediately reach a steady state, not evolving during ethylene or He flow (panels 2b and 2c), while the latter gradually increase in intensity in both conditions. Broad bands around 1590-1600 cm^{-1} have been typically observed in studies about coke formation, and have been assigned to polycondensed aromatics (coke or coke precursos) [29,35]. The band at 1505 (with shoulder at 1537 cm^{-1}) has a less straightforward explanation. Bands in similar positions have been reported and discussed by Pazè et al., who studied 1-butene interaction with H-Ferrierite [31]. The authors observed a band at 1500 cm^{-1} and acknowledged the fact that infrared alone cannot distinguish among the possible interpretations, which are in terms of a ν(C=C) mode of molecules having conjugated double bonds, such as aromatics and long-chain neutral and carbocationic alkenes. However, by combining UV-Vis spectroscopy to infrared, they assigned the signals between 1450 and 1550 cm^{-1} to enyl carbenium ions (with 2, 3 or more double bonds) and/or neutral di- and trienes [31]. Noticeably, Palumbo et al. could precisely assign a band

at 1520 cm^{-1} to cationic species, in relation to its disappearance upon NH_3 adsorption [36]. Based on our results, we are not able to assign the features at 1505 and 1537 cm^{-1} to a precise structure. However, based on the literature, and on the disappearance of the Brønsted signal, we can tentatively assign them to unsaturated carbocationic species, which are stabilized by the negative charges of the framework. Surprisingly, these bands continue growing after removing ethylene flow (Figure 2b), while no evident consumption of the other adsorbed species is observed. We could infer that this is related to a further reactivity of the adsorbed compounds, which change their structure. It is also worth noticing that the extinction coefficient of bands associated to carbocationic species is usually larger than that of the corresponding neutral species.

Upon increasing the temperature to 300 °C, the absorption bands related to the adsorbed saturated hydrocarbons gradually decrease in intensity, both in ethylene and He flow (Figure 2e,f). This can also be appreciated in Figure 4a, where the final states after He flow at each temperature are directly compared. In contrast, there is a growth in the intensity of the bands at 1597 and around 1500 cm^{-1}, particularly when increasing the temperature from 200 to 300 °C (compare intensities in panels d and e). This suggests that saturated hydrocarbons are desorbed, while carbocationic saturated species and coke/coke precursors are formed in greater amount. Notice that no bands are observed in the region of unsaturated $\nu(=CH_x)$ groups, suggesting that the formed species are highly alkylated.

Finally, most of the adsorbed species are desorbed heating up to 400 °C, and further decrease during He flow at the same temperature (Figure 2g,h). The most stable adsorbed species at this temperature are those responsible for the band at 1505 cm^{-1}, with a weak component at 1378 cm^{-1}, indicating that they are methylated molecules. This is in very good agreement with the work by Pazè et al, who showed a decrease of the band at 1500 cm^{-1}, assigned to enyl carbenium ions, while heating above 300 °C [31].

Figure 2. Background subtracted FT-IR spectra of H-ZSM5 sample recorded under ethylene (left) and helium (right) flow at different temperatures. Black curves were collected immediately after contact with ethylene or helium flows, grey curves were measured at intermediate time and coloured ones after 10 (ethylene, left) and 5 minutes (He, right). Arrows in each panel show the evolution with time of the main components. Coloured labels refer to gas phase ethylene bands.
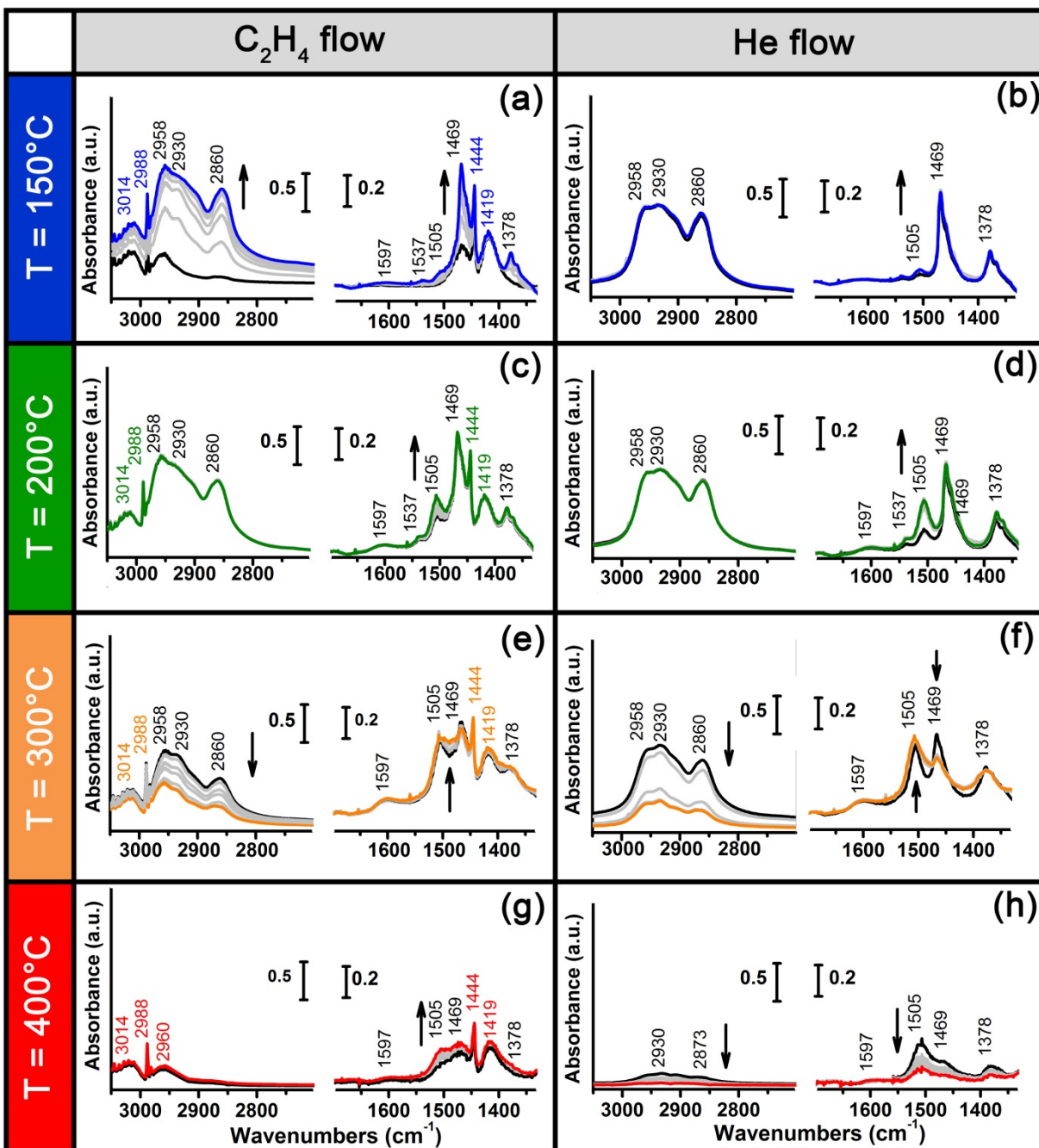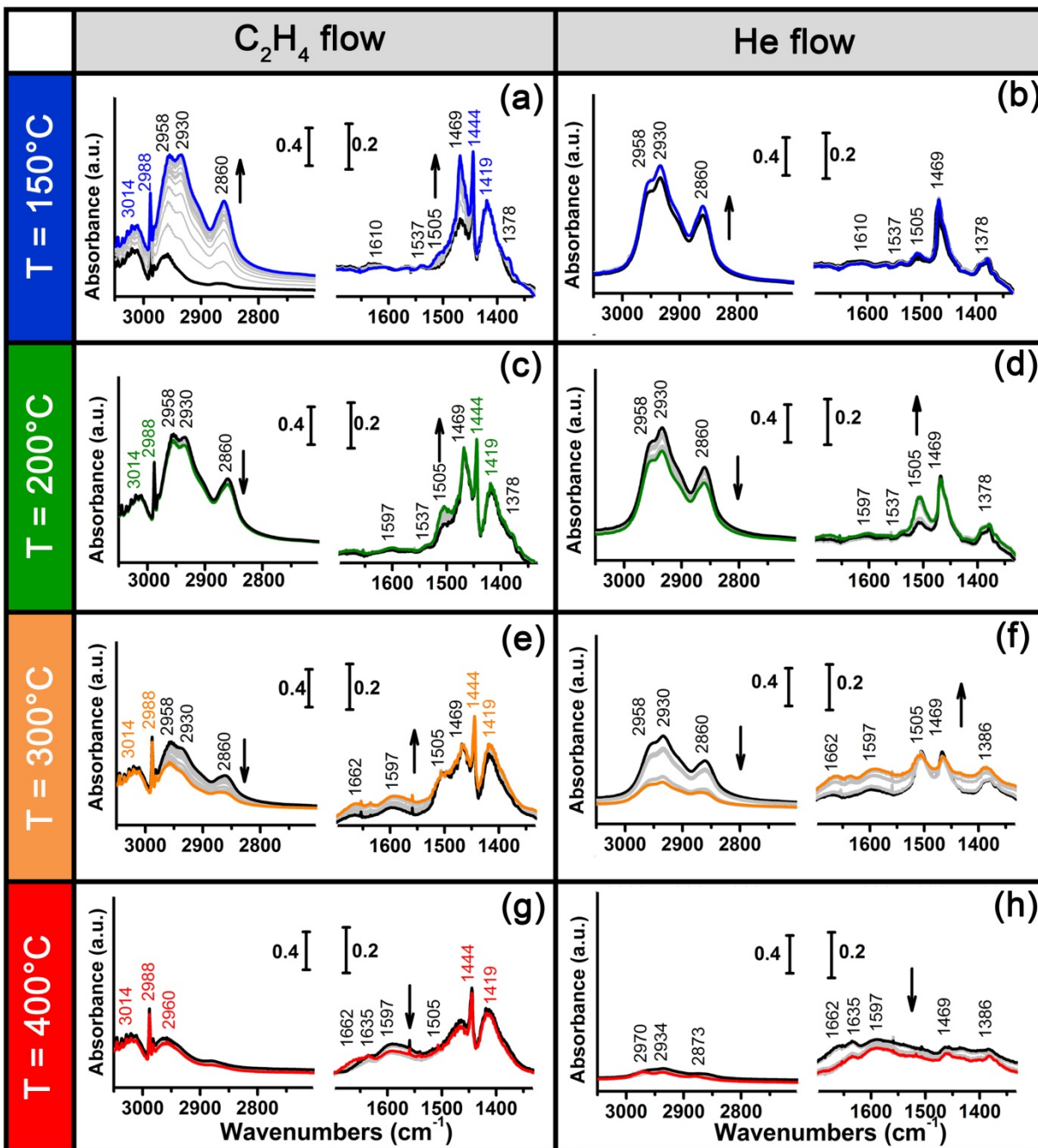
Figure 3. Background subtracted FT-IR spectra of Ni-ZSM5 sample recorded under ethylene (left) and helium (right) flow at different temperatures. Black curves were collected immediately after contact with ethylene or helium flows, grey curves were measured at intermediate time and coloured ones after 10 (ethylene, left) and 5 minutes (He, right). Arrows in each panel show the evolution with time of the main components. Coloured labels refer to gas phase ethylene bands.

The evolution of the FT-IR spectra of Ni-ZSM5 during ethylene and helium flows at different temperatures is shown in Figure 3. At 150 °C (Figure 3a,b) the main difference between H-ZSM5 and Ni-ZSM5 is the relative intensity of the CH$_3$ and CH$_2$ bands. The ν(CH$_3$) band at 2958 and the

$\delta(CH_3)$ band at 1378 cm^{-1} are relatively less intense with respect to the bands at 2930 and 1469 cm^{-1}, respectively. In other words, in the presence of Ni the adsorbed, mainly alkylated compounds show a relatively minor amount of methyl groups. Moreover, the $\delta(CH_3)$ band centred at 1378 cm^{-1}, shows additional components at higher and lower frequency (1390 and 1368 cm^{-1}), suggesting a variety of situations with carbon atoms linked to one, two or three methyl groups. Also in this case other weak features are observed at higher frequency. We acknowledge the fact that the relative intensity of the 1505 cm^{-1} band, tentatively assigned to unsaturated carbocations, is relatively higher with respect to what observed in H-ZSM-5 (see also Figure 4a, b right panels). These experimental evidences are in good agreement with the common belief that ethylene oligomerization on nickel sites occurs following a coordination catalysis mechanism, with ethylene inserting in a Ni-C bond, while the formed C4+ olefins might be consumed through isomerization and dimerization reactions on the Brønsted acid sites via a carbocationic mechanism. The whole process would lead to the formation of higher olefins, heavy branched, and of unsaturated carbocation intermediates, at the expenses of the Brønsted sites.

Upon increasing the temperature at 200 °C (Figure 3c,d) the intensity of the band at 1505 cm^{-1} increases, while no evident changes are observed in the coke/coke precursors region (1590-1600 cm^{-1}). A slightly faster decrease of the bands related to unsaturated groups is observed with respect to H-ZSM-5 (compare right panels of Figures 2d and 3d).

Major changes with respect to H-ZSM-5 are observed at 300 °C (Figure 3e,f and Figure 4). At this temperature, the species responsible for the band at 1505 cm^{-1} decreases (particularly when flushing with He), the broad band at 1597 cm^{-1} becomes evident and new broad features are formed at 1662 cm^{-1}, with a shoulder at 1635 cm^{-1}. This suggests that in the presence of Ni the adsorbed unsaturated carbocation are transformed in larger poly-condensed aromatics or aliphatic compounds. Indeed, broad and unresolved bands were observed during coke formation on H-ZSM-5 by Castaño et al., with maxima at 1640 and 1589 cm^{-1} [29]. Rozwadowsi et al. assigned a band at 1670 cm^{-1} to the $\nu(C=C)$ in alkenes [35], while Palumbo et al assigned a feature at 1690 cm^{-1} to $\nu(C=C)$ of cationic poly-conjugated species and one at 1620 cm^{-1} to $\nu(C=C)$ vibrational modes of a complex mixture of carbonaceous hydrogen-deficient species [36]. This spectral range is also typical for polyenes, with dienes and trienes expected in the 1670-1610 cm^{-1} interval [37]. Based on literature, we can safely assign the bands at 1597 and 1635 cm^{-1} to coke precursors formation. As for the band at 1662 cm^{-1} we cannot give a precise assignment. However, we tend to exclude that this is related to adsorbed oligomeric compounds (reaction products) since they only start to be observed at 400 °C. Moreover, this band is quite broad and unresolved, and is the only one increasing when flowing He at 400 °C (Figure 3h and 4b). This support the hypothesis that it is related to relatively large polycondensed unsaturated compounds. Noteworthy, in the $\nu(CH_x)$ stretching region no bands associable to unsaturated compounds are observed, although $\nu(CH_x)$ absorption bands are clearly present. These observations suggest that the entrapped species are highly methylated, and they slowly evolve into bigger compounds, ultimately leading to formation of coke-like species [36].

Finally, when reaching 400 °C, the most stable compounds are those related to unsaturated species and coke precursors (bands at 1662, 1635 and 1597 cm^{-1}), with weak features related to alkyl groups ($\nu(CH_x)$ and $\delta(CH_x)$ bands). Noticeably, the intensity of the band at 1505 cm^{-1}, assigned to unsaturated carbocations, is lower at this temperature with respect to what observed on H-ZSM-5. To conclude, the data shown in Figure 3 indicate that during ethylene oligomerization the presence of Ni Lewis sites [38] - in addition to Brønsted acid ones - favour the formation of larger, more complex and stable poly-condensed unsaturated hydrocarbons.
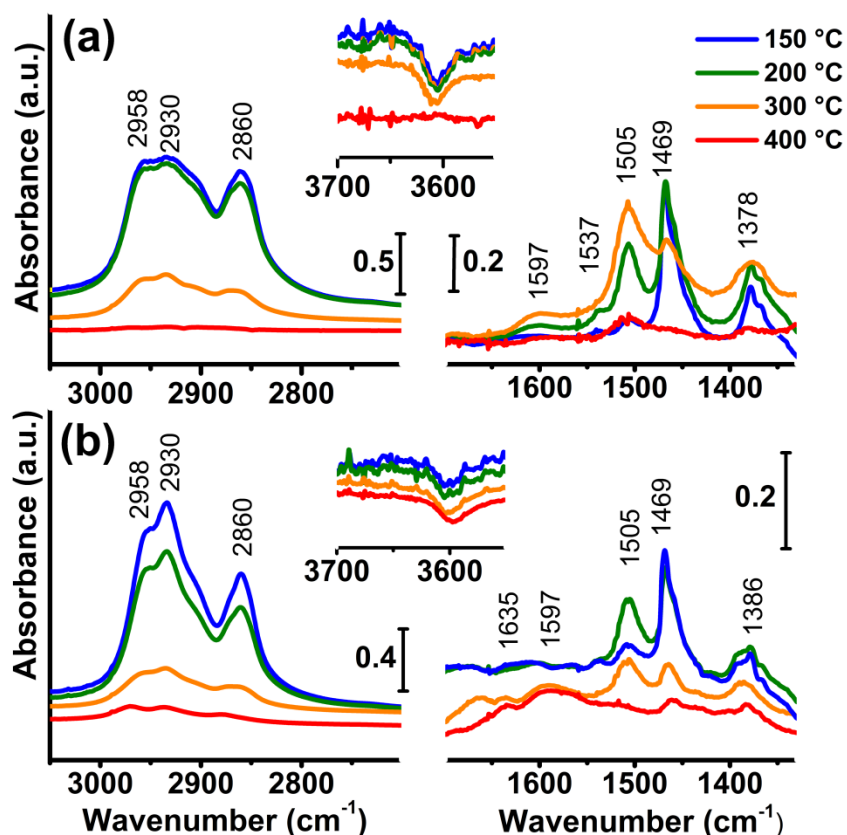

Figure 4. Summary of the FT-IR spectra of H-ZSM5 (part a) and Ni-ZSM5 (part b) catalysts measured under 5 minutes helium flow after ethylene contact, at different temperatures. The same code of colours used in Figures 2 and 3 is used. Insets show the corresponding $\nu(OH)$ region.

Figure 4 resumes the final FT-IR spectra collected at each temperature under helium flow for both H-ZSM5 and Ni-ZSM5 samples. For H-ZSM5, the spectra have some similarities to those reported in ref [29] (different coke species formed in a variety of zeolites during the cracking of polyethylene), and in ref. [36] (carbonaceous species formed in H-ZSM5 during methanol to aromatic conversion), and suggest the presence of alkylated compound, unsaturated carbocations and coke precursors. These species are almost entirely removed under helium flow at 400 °C. As a consequence, the absorption band due to the Brønsted sites almost recovers its initial intensity at 400 °C (negative band at ~3600 cm^{-1} almost disappears, see inset of Figure 4a). For Ni-ZSM5, different adsorbed compounds are observed since the beginning. These species are rapidly

converted into polycondensed unsaturated compounds, which remain adsorbed at the catalyst surface also under helium flow at 400 °C. Indeed, the absorption band due Brønsted sites is not restored even by heating in helium flow at 400 °C (see inset of Figure 4b). In other words, a complex mixture of poly-condensed aromatic species is formed. These are hard to be desorbed and they ultimately deactivate the catalyst.
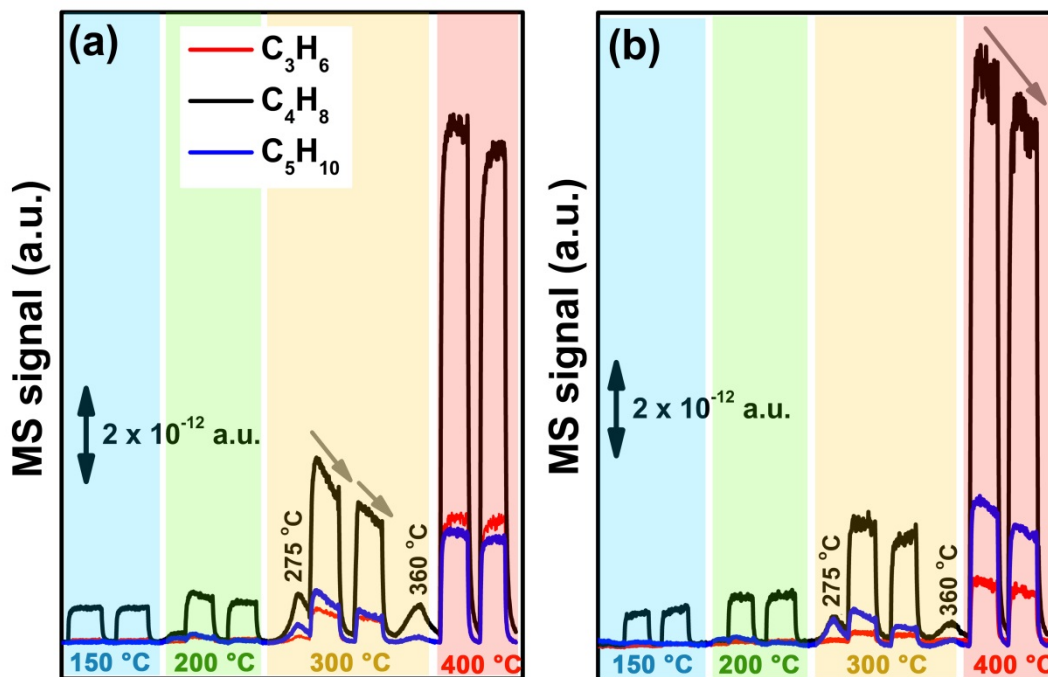

Figure 5. Mass spectra of output gases recorded on H-ZSM5 (left) and Ni-ZSM5 (right) catalysts during reaction with ethylene at different temperatures.

Figure 5 shows the MS data collected simultaneously to the FT-IR spectra during ethylene oligomerization on both H-ZSM5 and Ni-ZSM5 catalysts as a function of reaction temperature. Both catalysts already work at 150 °C (giving mainly butene product), although catalyst activity is maximized at 400 °C. These results are at variance with respect to literature, particularly in relation to the work by Lin et al. showing that H-ZSM 5 exhibited the highest activity for conversion of ethylene to products at 300 °C [18]. Also, it was shown that at low temperature (~ 300 °C) the main products for H-ZSM-5 are > C5 and aromatics, whereas at high temperatures (~ 500 °C) the main products are C3 and C4 olefins [18,39]. The differences with respect to literature could be related to the used experimental conditions, which in our case are not optimised for catalytic tests but for *in situ* spectroscopic studies. For both catalysts and at all temperatures, butene is the main reaction product, in agreement with literature, followed by pentene and propene [40]. At 300 °C both H-ZSM-5 and Ni-ZSM-5 shows an increase in activity. However, the product concentration rapidly decreases with time-on stream for H-ZSM-5, while this does not occur significantly for Ni-ZSM-5(see inset of Figure 5, left).

At 400 °C the behaviour is reversed: a faster decrease in the product concentration with time-on-stream is observed for i-ZSM-5 (inset of Figure 5, right). This can be related to the infrared observations, showing on this sample a relatively larger amount of adsorbed aliphatic and aromatic species (bands above 1500 cm^{-1}, compare panels h of Figures 2 and 3), which could be responsible for deactivation.

It is worth noticing that the same set of experiments described in the current work has also been performed on ZSM5 zeolites having different morphologies (nanosheet *vs* micron size particles) and different Ni insertion methods (ion exchange vs. incipient wetness impregnation). The catalysts properties and their preparation have been described in our earlier work [28]. Noticeably, the results obtained on nanosheet samples are identical to those obtained on commercial ZSM5 zeolite sample modified by nickel using the impregnation method (current work). This indicates that the deactivation mechanism and temperature are mainly related to the presence of nickel (high activity of Ni as Lewis acid sites) rather than to zeolite morphology or Ni insertion method.

Finally, we underline the fact that this work is mainly based on a spectroscopic evaluation of the stable adsorbed products, likely responsible for deactivation of the catalysts, addressing the role of Ni sites. This is a complex process, also in relation to the variety of Ni sites present in the catalyst, as a function of topology and insertion mechanism. For a more detailed description of the Ni sites present in the catalyst studied in this work interested readers are referred to our recent work, where the CO probe coupled to infrared spectroscopy was employed [28]. Moreover, the mechanism of ethylene oligomerization catalysed by Ni sites supported on porous materials is currently the subject of a lively debate. Main groups working on the subject include Lallemand et al. [21], Tanaka et al. [23] or Lehmann et al. [22]. Even if most of these authors propose Ni$^+$ as an active site, an increasing number of authors agree on the fact that Ni^{2+} is the active species [18,39]. For instance, Brogaard et al. proposed a mechanism for formation of active Ni-alkyl species between ethylene and isolated Ni^{2+} sites, showing by DFT that the most probable pathway is the Cossee-Arlam mechanism [19]. Finally, for a more detailed discussion about product distribution on bifunctional Ni-acid catalysts, interested readers are referred to the interesting work by Moussa et al. [41].

Conclusions

Ethylene oligomerization on H-ZSM5 and Ni-ZSM5 catalysts was investigated as a function of temperature by means of *in situ* FT-IR spectroscopy coupled with MS technique. It was found that the presence of nickel Lewis and redox acid sites greatly affects the amount and nature of the carbonaceous species adsorbed at the catalyst surface in working conditions. A complex mixture of poly-condensed aromatic (coke/coke precursors) are formed on Ni-ZSM5 and cannot be desorbed even at 400 °C, thus deactivating the catalyst. On the contrary, unsaturated carbocations, with a minor amount of poly-condensed methylated aromatic compounds are mainly formed on H-ZSM5, which could be readily desorbed at 400 °C. These results allow to rationalize at least in

part the catalysts deactivation mechanism. On these basis, it is proposed that zeolites with larger pore diameter (such as H-beta [38], to increase the desorption rate of surface species) or with additional metal ions (to decrease the activity of the nickel sites) might inhibit catalyst deactivation.

As a final remark, we believe that the presented results are unique, since they compare the chemistry taking place in the same experimental conditions at the surface of two catalysts having the same physico-chemical properties but differing because of the presence or absence of Ni sites. Although this work cannot be considered as an *operando* study (since we are working at ambient pressure at variance with real catalytic tests) it allows us to pinpoint the influence of Ni sites on the reactivity towards ethylene oligomerization.

References

1. Al-Jarallah A, Anabtawi J, Siddiqui M, Aitani A, Al-Sa'doun A (1992) Ethylene dimerization and oligomerization to butene-1 and linear α-olefins: a review of catalytic systems and processes. Catalysis Today 14 (1):1-121.
2. Agapie T (2011) Selective ethylene oligomerization: Recent advances in chromium catalysis and mechanistic investigations. Coordination Chemistry Reviews 255 (7–8):861-880.
3. Finiels A, Fajula F, Hulea V (2014) Nickel-based solid catalysts for ethylene oligomerization–a review. Catalysis Science & Technology 4 (8):2412-2426.
4. O'Connor CT, Kojima M (1990) Alkene oligomerization. Catalysis Today 6 (3):329-349.
5. Svejda SA, Brookhart M (1999) Ethylene Oligomerization and Propylene Dimerization Using Cationic (α-Diimine)nickel(II) Catalysts. Organometallics 18 (1):65-74.
6. Chen Y, Qian C, Sun J (2003) Fluoro-Substituted 2,6-Bis(imino)pyridyl Iron and Cobalt Complexes: High-Activity Ethylene Oligomerization Catalysts. Organometallics 22 (6):1231-1236.
7. Lallemand M, Finiels A, Fajula F, Hulea V (2006) Catalytic oligomerization of ethylene over Ni-containing dealuminated Y zeolites. Applied Catalysis A: General 301 (2):196-201.
8. Fischer K, Jonas K, Misbach P, Stabba R, Wilke G (1973) The "Nickel Effect". Angewandte Chemie International Edition in English 12 (12):943-953.
9. Keim W (2013) Oligomerization of Ethylene to α-Olefins: Discovery and Development of the Shell Higher Olefin Process (SHOP). Angewandte Chemie International Edition 52 (48):12492-12496.
10. Yamamura M, Chaki K, Wakatsuki T, Okado H, Fujimoto K (1994) Synthesis of ZSM-5 zeolite with small crystal size and its catalytic performance for ethylene oligomerization. Zeolites 14 (8):643-649.
11. Böhme U, Barth B, Paula C, Kuhnt A, Schwieger W, Mundstock A, Caro Jr, Hartmann M (2013) Ethene/ethane and propene/propane separation via the olefin and paraffin selective metal–organic framework adsorbents CPO-27 and ZIF-8. Langmuir 29 (27):8592-8600.
12. Kulprathipanja S (2010) Zeolites in Industrial Separation and Catalysis. Wiley-VCH, Weinheim
13. Aguado S, Bergeret G, Daniel C, Farrusseng D (2012) Absolute Molecular Sieve Separation of Ethylene/Ethane Mixtures with Silver Zeolite A. Journal of the American Chemical Society 134 (36):14635-14637.
14. Xi J, Miao S, Tang X (2004) Selective transporting of lithium ion by shape selective molecular sieves ZSM-5 in PEO-based composite polymer electrolyte. Macromolecules 37 (23):8592-8598.
15. Hartmann M, Pöppl A, Kevan L (1996) Ethylene dimerization and butene isomerization in nickel-containing MCM-41 and AlMCM-41 mesoporous molecular sieves: an electron spin resonance and gas chromatography study. The Journal of Physical Chemistry 100 (23):9906-9910.
16. Hulea V, Fajula F (2004) Ni-exchanged AlMCM-41—An efficient bifunctional catalyst for ethylene oligomerization. Journal of Catalysis 225 (1):213-222.
17. Lallemand M, Rusu OA, Dumitriu E, Finiels A, Fajula F, Hulea V (2008) NiMCM-36 and NiMCM-22 catalysts for the ethylene oligomerization: Effect of zeolite texture and nickel cations/acid sites ratio. Applied Catalysis A: General 338 (1):37-43.
18. Lin B, Zhang Q, Wang Y (2009) Catalytic Conversion of Ethylene to Propylene and Butenes over H−ZSM-5. Industrial & Engineering Chemistry Research 48 (24):10788-10795.
19. Brogaard RY, Olsbye U (2016) Ethene Oligomerization in Ni-containing Zeolites: Theoretical Discrimination of Reaction Mechanisms. ACS Catalysis 6:1205–1214.
20. Speiser F, Braunstein P, Saussine L (2005) Catalytic Ethylene Dimerization and Oligomerization: Recent Developments with Nickel Complexes Containing P,N-Chelating Ligands. Accounts of Chemical Research 38 (10):784-793.
21. Zhang Q, Kantcheva M, Dalla Lana IG (1997) Oligomerization of ethylene in a slurry reactor using a nickel/sulfated alumina catalyst. Industrial & engineering chemistry research 36 (9):3433-3438.

22. Lallemand M, Finiels A, Fajula Fo, Hulea V (2009) Nature of the Active Sites in Ethylene Oligomerization Catalyzed by Ni-Containing Molecular Sieves: Chemical and IR Spectral Investigation. The Journal of Physical Chemistry C 113 (47):20360-20364.

23. Lehmann T, Wolff T, Zahn VM, Veit P, Hamel C, Seidel-Morgenstern A (2011) Preparation of Ni-MCM-41 by equilibrium adsorption — Catalytic evaluation for the direct conversion of ethene to propene. Catalysis Communications 12 (5):368-374.

24. Tanaka M, Itadani A, Kuroda Y, Iwamoto M (2012) Effect of Pore Size and Nickel Content of Ni-MCM-41 on Catalytic Activity for Ethene Dimerization and Local Structures of Nickel Ions. The Journal of Physical Chemistry C 116 (9):5664-5672.

25. Gurlo A, Riedel R (2007) In situ and operando spectroscopy for assessing mechanisms of gas sensing. Angewandte Chemie International Edition 46 (21):3826-3848.

26. Topsøe H (2003) Developments in operando studies and in situ characterization of heterogeneous catalysts. Journal of Catalysis 216 (1):155-164.

27. Stepanov AG, Luzgin MV, Romannikov VN, Sidelnikov VN, Paukshtis EA (1998) The Nature, Structure, and Composition of Adsorbed Hydrocarbon Products of Ambient Temperature Oligomerization of Ethylene on Acidic Zeolite H-ZSM-5. Journal of Catalysis 178 (2):466-477.

28. Ganjkhanlou Y, Groppo E, Bordiga S, Volkova MA, Berlier G (2016) Incorporation of Ni into HZSM-5 zeolites: Effects of zeolite morphology and incorporation procedure. Microporous and Mesoporous Materials 229:76-82.

29. Castaño P, Elordi G, Olazar M, Aguayo AT, Pawelec B, Bilbao J (2011) Insights into the coke deposited on HZSM-5, Hβ and HY zeolites during the cracking of polyethylene. Applied Catalysis B: Environmental 104 (1):91-100.

30. Spoto G, Bordiga S, Ricchiardi G, Scarano D, Zecchina A, Borello E (1994) IR study of ethene and propene oligomerization on H-ZSM-5: hydrogen-bonded precursor formation, initiation and propagation mechanisms and structure of the entrapped oligomers. J Chem Soc, Faraday Trans 90 (18):2827-2835.

31. Pazè C, Sazak B, Zecchina A, Dwyer J (1999) FTIR and UV− Vis Spectroscopic Study of Interaction of 1-Butene on H− Ferrierite Zeolite. The Journal of Physical Chemistry B 103 (45):9978-9986.

32. Bolis V, Vedrine JC, Van de Berg JP, Wolthuizen JP, Derouane EG (1980) Adsorption and activation of ethene by zeolite-H-ZSM-5. Journal of the Chemical Society, Faraday Transactions 1: Physical Chemistry in Condensed Phases 76:1606-1616.

33. Groppo E, Lamberti C, Bordiga S, Spoto G, Zecchina A (2006) In situ FTIR spectroscopy of key intermediates in the first stages of ethylene polymerization on the Cr/SiO 2 Phillips catalyst: Solving the puzzle of the initiation mechanism? Journal of Catalysis 240 (2):172-181.

34. Trombetta M, Busca G, Rossini SA, Piccoli V, Cornaro U (1997) FT-IR Studies on Light Olefin Skeletal Isomerization Catalysis: I. The Interaction of C4 Olefins and Alcohols with Pure γ-Alumina. Journal of Catalysis 168 (2):334-348.

35. Rozwadowski M, Lezanska M, Wloch J, Erdmann K, Golembiewski R, Kornatowski J (2001) Investigation of coke deposits on Al-MCM-41. Chemistry of materials 13 (5):1609-1616.

36. Palumbo L, Bonino F, Beato P, Bjørgen M, Zecchina A, Bordiga S (2008) Conversion of Methanol to Hydrocarbons: Spectroscopic Characterization of Carbonaceous Species Formed over H-ZSM-5. The Journal of Physical Chemistry C 112 (26):9710-9716.

37. Socrates G (2004) Infrared and Raman characteristic group frequencies: tables and charts. John Wiley & Sons, Chichester

38. Martínez A, Arribas MA, Concepción P, Moussa S (2013) New bifunctional Ni–H-Beta catalysts for the heterogeneous oligomerization of ethylene. Applied Catalysis A: General 467:509-518.

39. Van den Berg J, Wolthuizen J, Van Hooff J (1983) Reaction of small olefins on zeolite H-ZSM-5. A thermogravimetric study at low and intermediate temperatures. Journal of Catalysis 80 (1):139-144.

40. Reddy JK, Motokura K, Koyama T-r, Miyaji A, Baba T (2012) Effect of morphology and particle size of ZSM-5 on catalytic performance for ethylene conversion and heptane cracking. Journal of Catalysis 289:53-61.

41. Moussa S, Arribas MA, Concepción P, Martínez A (2016) Heterogeneous oligomerization of ethylene to liquids on bifunctional Ni-based catalysts: The influence of support properties on nickel speciation and catalytic performance. Catalysis Today 277:78-88.